Two-dimensional analogs of the H_2^+ ion in stationary electric fields

Mikhail V. Ivanov* and Reinhard Schinke
Max-Plank-Institut für Strömungsforschung, Bunsenstrasse 10, D-37073 Göttingen, Federal Republic of Germany
(Received 9 July 2003; published 12 April 2004)

We calculate energies and lifetimes for two two-dimensional analogs of the hydrogen molecular ion H_2^+ in external static electric fields directed along the axis of the system. They are two positive Coulomb impurity centers with one electron in a narrow two-dimensional quantum well and the electron in a double quantum dot. For state $2p\sigma_u$ we obtain oscillating dependencies of the ionization rate Γ on the electric-field strength F and the distance between centers R. We explain the oscillation picture by an interference of the electronic wave between two centers. The oscillations decrease faster for a pair of quantum dots with short-range attractive potentials than for a pair of Coulomb centers. The latter is due to the fact that long-range Coulomb potentials form a kind of channel preventing a dissipation of the electronic density sidewards from the axis of the system.

DOI: 10.1103/PhysRevB.69.165308 PACS number(s): 73.63.Kv, 73.50.Fq, 73.23.Hk, 33.55.Be

I. INTRODUCTION

The properties of both neutral and charged donors in narrow quantum wells are a subject of considerable interest during several decades.[1–8] In very narrow wells a neutral donor can be considered as a two-dimensional (2D) analog of the hydrogen atom. A frequently used compound for experimental investigations (see, for example, Refs. 7 and 8) of such systems is layers of GaAs/AlGaAs. The high mobility, i.e., small effective mass of electrons and the comparatively large dielectricity constant of this and many other semiconductor materials, facilitate to study strong electric-field effects in the laboratory. Investigations of quantum dots of various origins including their behavior in external electric fields is also a point of many experimental and theoretical works. An investigation of the electronic properties of ensembles of donors or quantum dots is natural in this context. Effects of electric fields on these ensembles can affect various properties of semiconductors including their conductivity.

In this work we restrict ourselves to the simplest ensemble of two quantum dots or two Coulomb impurity centers and consider the behavior of an electron in such a system.

In this formulation the problem is a close analog to the problem of the hydrogen molecular ion H_2^+ in an electric field. The latter problem was investigated in recent years and a number of interesting physical results were reported. The most impressive results were obtained for electric fields parallel to the molecular axis. They are the oscillating dependencies of the ionization rate Γ of the state $2p\sigma_u$ on the electric-field strength F and the internuclear distance R. These dependencies are clearly visible in Fig. 5 of Refs. 9. To get a better basis for comparison of 2D and 3D cases following in next sections we provide in Fig. 1 our result for the hydrogen molecular ion, obtained by a solution of the corresponding 3D Schrödinger equation by the method described in the following section and in Refs. 10. Most of existing interpretations of this phenomenon[9,11–13] address one or two major maxima of the ionization rate Γ to an interaction of a quasistationary state localized at one of the nuclei with broad resonance states at the second one. However, this argumentation does not explain the nearly periodic character of the function $\Gamma(R)$ and the decrease of its period with F. A different point of view on this phenomenon, based on an analysis of a phase of the wave function, is presented in Ref. 14. But all the calculations of the latter work are carried out for a simple one-dimensional model. These details concerning the H_2^+ ion were an additional reason for investigating two-dimensional systems, similar to H_2^+.

II. FORMULATION OF THE PROBLEM AND THE METHOD OF SOLUTION

The Schrödinger equation for an electron confined in the plane (x,y) and moving in the field of two Coulomb centers at points $(-R/2,0)$ and $(R/2,0)$ and a constant uniform electric field F pointing along the x direction is given by

$$\left[-\frac{\hbar^2}{2\mu m_0}\left(\frac{\partial^2}{\partial x^2}+\frac{\partial^2}{\partial y^2}\right)-\frac{e^2}{\kappa\sqrt{(x+R/2)^2+y^2}}-\frac{e^2}{\kappa\sqrt{(x-R/2)^2+y^2}}-|e|Fx\right]\psi=E\psi, \tag{1}$$

where μ is the effective mass of the electron in m_0 units, κ is the dielectric constant, and e is the charge of the electron. Positions E_0 and half-widths $\Gamma/2$ of resonances can be obtained from complex eigenvalues of the energy $E=E_0-i\Gamma/2$. These eigenvalues have to correspond to solutions of Eq. (1) having the asymptotics of an outgoing wave. At the same time the value $1/\Gamma$ gives the average lifetime of corresponding quasistationary states. Equation (1) can be rewritten in effective atomic units as

$$\left[-\frac{1}{2}\left(\frac{\partial^2}{\partial x^2}+\frac{\partial^2}{\partial y^2}\right)-\frac{1}{\sqrt{(x+R/2)^2+y^2}}-\frac{1}{\sqrt{(x-R/2)^2+y^2}}-Fx\right]\psi=E\psi. \tag{2}$$

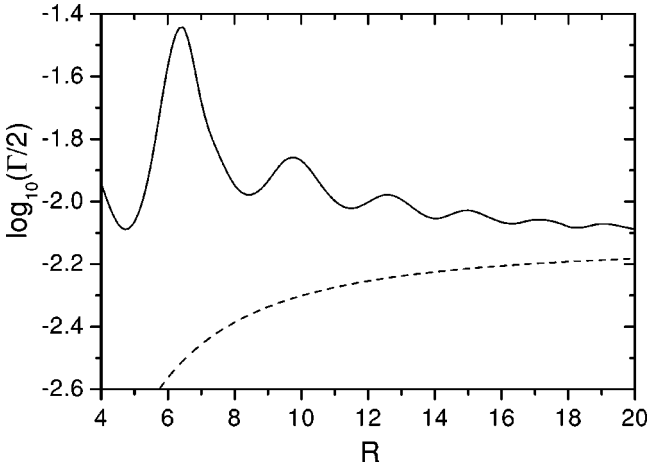

FIG. 1. Half-widths of levels $1s\sigma_g$ (dashed line) and $2p\sigma_u$ (solid line) of the hydrogen molecular ion H_2^+ in a longitudinal electric field $F=0.1$ as functions of the internuclear distance R. Atomic units.

The units of energy, length, field strength, and time are $\mu\kappa^{-2}(27.2)$ eV, $\kappa\mu^{-1}(5.29\times10^{-9})$ cm, $\mu^2\kappa^{-3}(5.14\times10^{9})$ V/cm, and $\kappa^2\mu^{-1}(2.42\times10^{-17})$ sec. When we consider a case of two quantum dots possessing non-Coulombic attractive potentials $V(x,y)$, we have to substitute the two first potential terms in Eq. (2) by an expression

$$V(x+R/2,y)+V(x-R/2,y). \tag{3}$$

For $F>0$ the external electric field destroys the symmetry between the two centers. In result, the potential energy of the electron in the vicinity of the center $(-R/2,0)$ becomes, generally speaking, higher than in the corresponding vicinity of the center $(R/2,0)$. In the following we have to distinguish these two Coulomb centers. To this end we refer to the center at $(-R/2,0)$ as to the upper one, and the center at $(R/2,0)$ will be noted as the lower one.

Useful information for the limits $R\to\infty$ and $R\to0$ can be obtained from solutions of an equation for a one-center problem,

$$\left[-\frac{1}{2}\left(\frac{\partial^2}{\partial x^2}+\frac{\partial^2}{\partial y^2}\right)-\frac{Z}{r}-Fx\right]\psi=E\psi, \tag{4}$$

where Z is the charge of the Coulomb center and $r=(x^2+y^2)^{1/2}$. For $F=0$ this equation has well-known analytic solutions[15] with energy levels forming a 2D Coulomb series with energies

$$E_n=-\frac{Z^2}{2(n-1/2)^2}, \tag{5}$$

where $n=1,2,3,\ldots$. Numerical solutions of Eq. (4) for $F>0$ are obtained in Ref. 16 for $Z=1$. Results for other Z values can be easily obtained by means of a scaling relation

$$E(Z,F)=Z^2E(1,F/Z^3). \tag{6}$$

The spatial coordinates are scaled in this situation as $x(Z,F)=x(1,F/Z^3)/Z$.

We have solved Eq. (2) by a multidimensional finite-difference method. It is presented in detail in Refs. 17–19 (bound states, see also its applications for Hartree-Fock calculations of atoms in strong magnetic fields[20,21] and for some other systems[22,23]) and in Refs. 10 and 24–26 (quasistationary states in external electric fields).

The applications in electric fields include the first calculation of energies and half-widths of levels of the H_2^+ molecular ion[24] and detailed calculations for the hydrogen atom in parallel electric and magnetic fields.[10] In Refs. 10 and 24–26 we have developed different approaches for calculation of wave functions with the asymptotics of an outgoing wave. Two of these approaches, i.e., a boundary condition method[24,25] and smooth exterior complex scaling,[10] are applicable for the two-center problem considered here. For most of the calculations presented below we used the smooth exterior complex scaling, which provides essential advantages in the calculations.

In contrast to variational calculations we are not restricted by using a particular ansatz for the wave function but perform a full grid solution to the Schrödinger equation that allows us to control and to estimate the remaining minor deviations from the exact eigenfunctions and eigenvalues. One of elements of this control consists in employing the Richardson's procedure,[18] which provides a reliable estimation of numerical errors.

Equation (2) was solved on rectangular meshes in Cartesian coordinates (x,y). A typical size of meshes in the present calculations for Coulomb centers was, e.g., 100 nodes in the y direction and 3000 in the x direction. The number of nodes for the x coordinate depends on the electric-field strength and increases with decreasing F values. Thus, the meshes contain more nodes than those used in our calculations of 3D systems.[10,24–26] The difference is due to higher effect of Coulomb singularities on the precision of calculations in 2D Schrödinger equations compared to 3D ones. This effect could be roughly evaluated as

$$\delta E\approx\int_{\Omega_0}\frac{1}{r}|\psi|^2dV,$$

where the region Ω_0 is, e.g., a circle (2D) or a sphere (3D) of a radius r_0 centered at the singularity. If $|\psi|^2$ does not vanish as $r_0\to0$, then $\delta E=O(r_0^2)$ in a 3D case and $O(r_0^1)$ in 2D. Therefore, in the present calculations we need thicker meshes to achieve the same precision as in the 3D case. The second reason for using thicker meshes is the numerical representation of fast oscillating wave functions. As one can see in the following sections, this is especially important for large R values.

III. TWO COULOMB CENTERS

In Fig. 2 we present a plot of the potential energy of an electron for two different central potentials V considered in this paper. For a system of two Coulomb centers (2) presented in this section we show also the positions of the $1s\sigma_g$

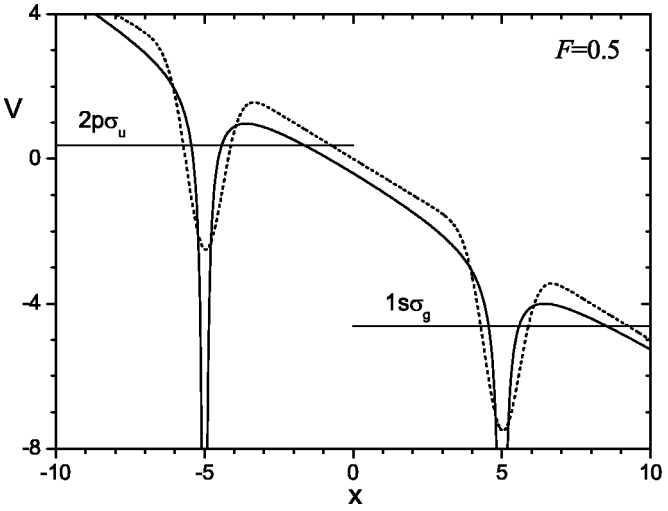

FIG. 2. Potential energy of an electron in a two-dimensional two-center system at $R=10$, $F=0.5$, and $y=0$ for two Coulomb centers (solid lines) and two Gaussian potential wells (dotted line). The horizontal lines present the real parts of energies of the $1s\sigma_g$ and $2p\sigma_u$ levels in the system of two Coulomb centers. Effective atomic units.

and $2p\sigma_u$ levels. At $F=0$ and large (but finite) distances R between the centers the level $2p\sigma_u$ lies somewhat higher than the ground state $1s\sigma_g$. As $R\to\infty$ these states become degenerate. Their wave functions have equal densities at $F=0$ in the vicinities of both centers. The difference between these two wave functions is that the wave function of the $1s\sigma_g$ has no zeros, whereas the wave function of the $2p\sigma_u$ changes its sign at $x=0$. The corresponding states at $F>0$ can be referenced according to a noncrossing rule. As a result, the ground state retains the name $1s\sigma_g$. For not very small R and F values the corresponding electronic density is concentrated practically around the right (the lower) center in Fig. 2. On the other hand, the electronic density of the state $2p\sigma_u$ concentrates near the left (the upper) Coulomb center.

Our results for the two states $1s\sigma_g$ and $2p\sigma_u$ are presented in the following figures. In the upper panel of Fig. 3 we depict the real parts of the energy of these states for a broad range of electric-field strengths. For the electronic states $1s\sigma_g$ and $2p\sigma_u$ these field strengths correspond both to the regime of underbarrier tunneling of the electron ($F\leqslant 1$) and to the overbarrier regime ($F>1$) for the electron leaving the system. For $R>3$ the functions $E_0(R)$ form an evident fanlike picture, corresponding to the two ground states of the electron in separate potential wells. For $R<1$ these dependencies correspond to the ground and a excited states of the united system. In the region between $R=1$ and $R=3$ one can see a picture of a transformation between these two scenarios. All the dependencies $E_0(R)$ for the $1s\sigma_g$ state for large R values do not reveal any deviations from linearity. The same takes place for the state $2p\sigma_u$ at fields corresponding to the regime of tunneling. On the other hand, for strong electric fields the dependencies of the real part of the energy of the state $2p\sigma_u$ contain oscillations, corresponding much more visible oscillations of the imaginary part of the energy of this state, presented in the lower panel of Fig. 3.

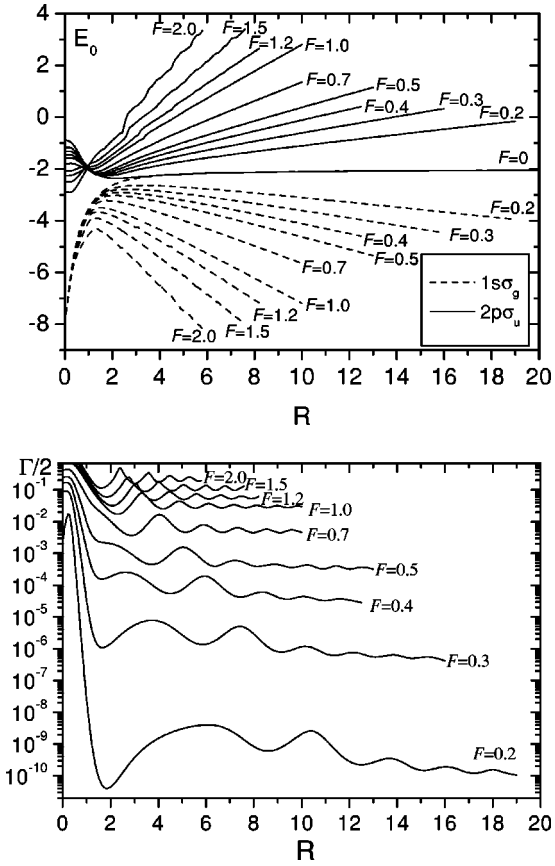

FIG. 3. Real and imaginary parts of the energy of an electron in a two-dimensional system of two Coulomb centers as functions of the distance R between the centers for various electric-field strengths. States $1s\sigma_g$ and $2p\sigma_u$. Effective atomic units.

These oscillations are the most interesting feature of the functions $\Gamma/2(R)$. Their presence does not depend on the electric-field strength including both regimes of the underbarrier tunneling and overbarrier ionization. The whole range

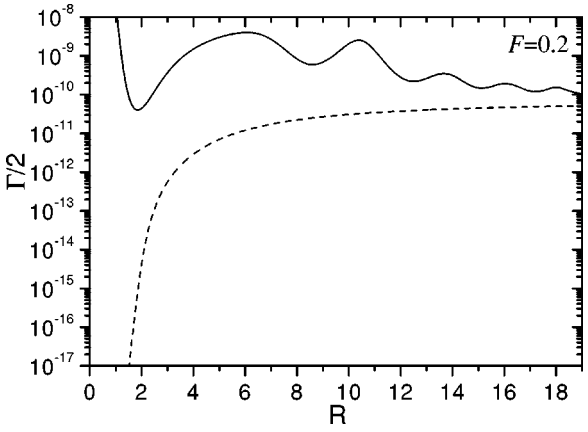

FIG. 4. Imaginary parts of energies of states $1s\sigma_g$ (dashed line) and $2p\sigma_u$ (solid line) in a two-dimensional system of two Coulomb centers as functions of the distance R between centers $F=0.2$. Effective atomic units.

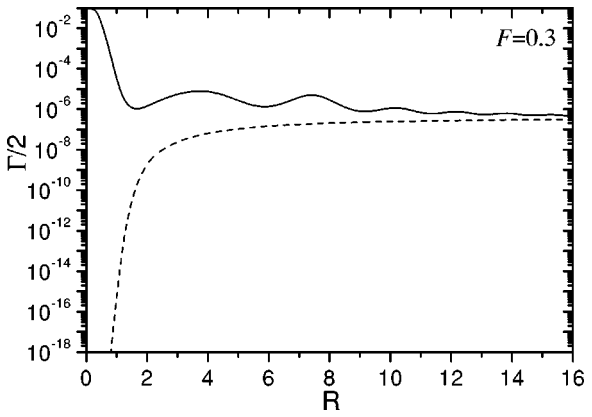

FIG. 5. Same as Fig. 4 for $F=0.3$.

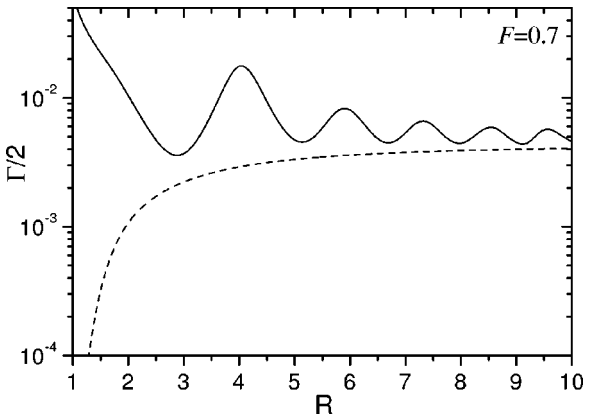

FIG. 7. Same as Fig. 4 for $F=0.7$.

of $\Gamma/2$ in the lower panel of Fig. 3 covers more than ten decimal orders. In comparison with the real part of the energy the values and oscillations of $\Gamma/2$ are negligibly small for small F values. This explains the absence of visible oscillations of the real part of the energy for relatively weak electric fields. On the other hand, at strong electric fields the real and imaginary parts of the energy have comparable magnitudes and the oscillations of $\Gamma/2$ are reflected in the behavior of $E_0(R)$. For each separate value of the electric-field strength the amplitude of oscillations decreases with increasing R values. In the limit of infinitely separate centers the value $\Gamma/2$ for the state $2p\sigma_u$ tends to the value, which is characteristic for the ground state of a separate center and dependent on F values. Numerical values for this limit are given in Ref. 16. This feature is more visible in Figs. 4–11, where we present $\Gamma/2(R)$ for both $2p\sigma_u$ and $1s\sigma_g$ states. The data in Figs. 4–11 are presented on various scales that allow one to see different details of the behavior of functions $\Gamma/2(R)$ for these two states.

Opposite to the state $2p\sigma_u$ the function $\Gamma/2(R)$ for the state $1s\sigma_g$ has no oscillations and reveals only a sharp decrease as $R\to 0$ and a slow convergence to a limit as $R\to\infty$. The first feature is associated with a sharp growth of the binding energy of the electron as $R\to 0$. (For $F=0$ and $R=0$ the energy of the ground state is -8 a.u. in contrast to $E=-2$ a.u. for $R=\infty$). An increase of $\Gamma/2$ for state $2p\sigma_u$ as $R\to\infty$ has an analogous origin and results from decreasing the binding energy of this excited state in the limit of the ''united atom.'' A slow convergence of $\Gamma/2$ for the state $1s\sigma_g$ to the limit $R\to\infty$ results from the long-range character of the Coulomb potential and a slow decrease of the influence of the neighboring (upper) center as $R\to\infty$.

One can see in Fig. 3 that the oscillations of $\Gamma/2$ for different F form a regular picture, so that it is possible to identify corresponding maxima and minima of the $\Gamma/2(R)$ for different F values. Aside from the decrease of the amplitude of oscillations of $\Gamma/2(R)$ for state $2p\sigma_u$ with increasing R the important feature of these functions is a decrease of the period of the oscillations with increasing R and F values. The latter feature leads to more and more sharp maxima and minima in the corresponding plots when increasing the electric-field strength. These features are good visible in Figs. 3–12. Rather similar features can be seen for a hydrogen molecular ion H_2^+ in Fig. 1 and in special works in the literature addressing directly this problem.[9,11–13] A picture similar to Fig. 3 can be seen in Ref. 9 (Figs. 3 and 5). The main difference between the 3D hydrogen molecular ion, considered in the cited papers, and its 2D analog, which we study here, consists in faster decrease of the oscillations of $\Gamma/2$ at large R in the 3D system. This difference can be seen in Fig. 11. Along with 2D curves for $F=F_{2D}=2$ we present

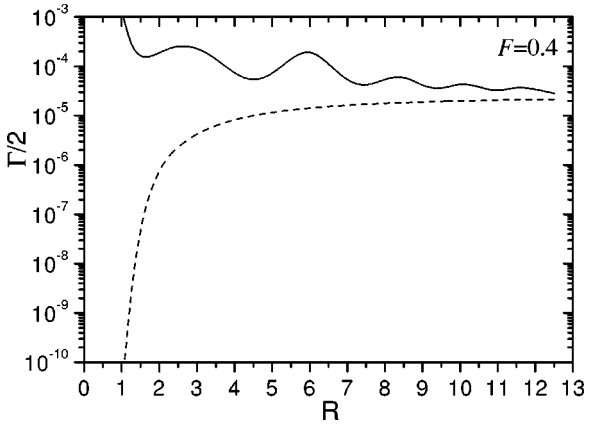

FIG. 6. Same as Fig. 4 for $F=0.4$.

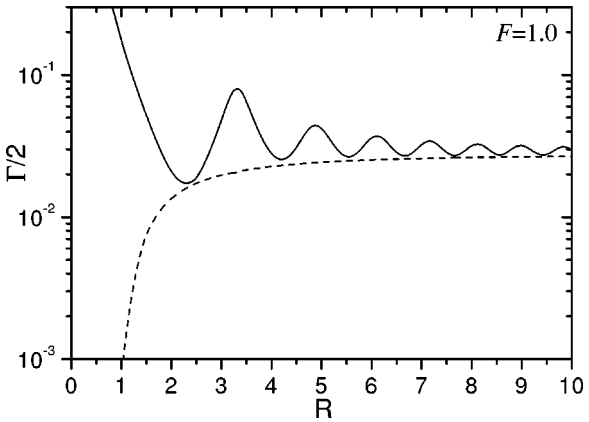

FIG. 8. Same as Fig. 4 for $F=1.0$.

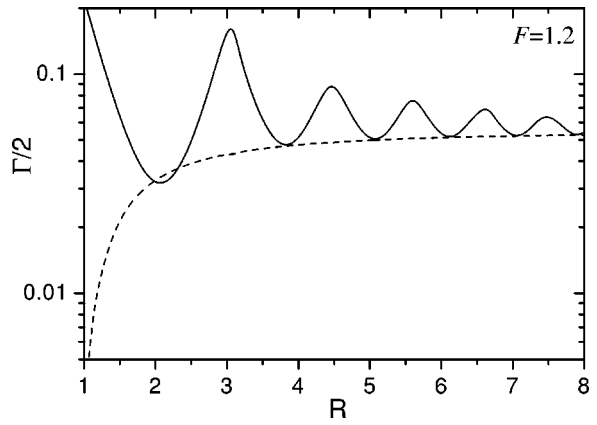

FIG. 9. Same as Fig. 4 for $F=1.2$.

in this figure a curve for state $2p\sigma_u$ of the 3D hydrogen molecule. Due to different binding energies of the electron in 2D and 3D systems the characteristic electric-field strengths providing similar effects are different for these systems. In order to make 2D and 3D dependencies comparable the latter have to be scaled. It is possible to do this by means of relation (6) with a formal parameter $Z=(F_{2D}/F_{3D})^{1/3}$. In Fig. 11 we give the 3D curve for $F_{3D}=0.1$. Comparing to Fig. 1 the Γ values in Fig. 11 have an additional multiplier $20^{2/3}$ whereas the R values are multiplied by $20^{-1/3}$.

The faster distinguishing of oscillations and maybe lower precision of calculations could make conditions for explaining only the first of the maxima in curves $\Gamma(R)$ in papers, cited above (two first maxima in Ref. 9). The explanation was based on a conjecture that a separate Coulomb potential well has broad resonances lying at relatively high energies and the maxima take place at points of intersections of real parts of energies of these resonances with the relatively narrow level $2p\sigma_u$. Such an explanation can be very reasonable in many cases, but it does not explain two or three major features of the picture obtained for the hydrogen molecular ion and its two-dimensional analogs. They are the periodicity of maxima and minima, the sine-shaped form of dependencies for large R values, and the fact that the period of the oscillations decreases whereas the maxima become narrower with increasing the electric-field strength. It should be noted that if the cited hypothesis were true, the shape of maxima

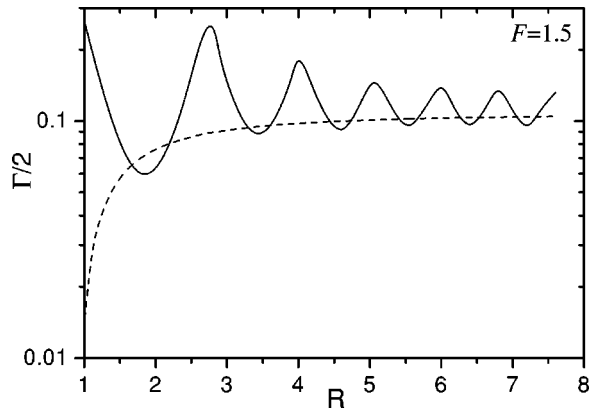

FIG. 10. Same as Fig. 4 for $F=1.5$.

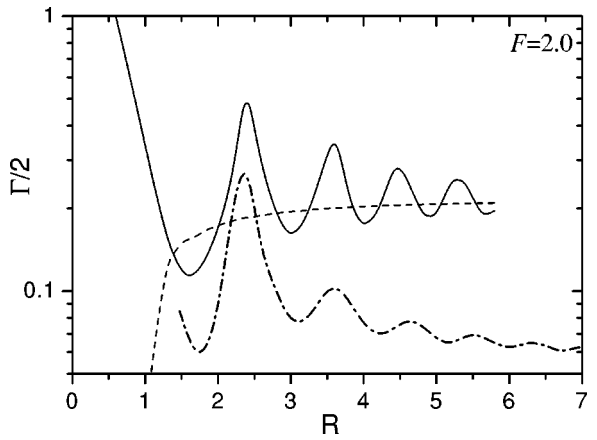

FIG. 11. Solid and dashed lines are same as Fig. 4 for $F=2.0$. Dash-dotted line is scaled ($R'=20^{-1/3}R$, $\Gamma'=20^{2/3}\Gamma$) dependence $\Gamma/2(R)$ for state $2p\sigma_u$ (dash-dotted line) of the 3D hydrogen molecular ion for $F=0.1$. Effective atomic units.

should correspond to the shape of the broad resonances at the lower potential well. Thus, as one can see in Fig. 3 these resonances must be very broad at small F and become narrower when increasing the electric-field strength. Moreover, our results allow one to obtain that the widths of all these resonances are to be proportional to the value $\sqrt{F}$. This contradicts a well-known picture for both a hydrogen atom in strong electric fields,[27–29,31] which is actual for the hydrogen molecular ion, and for a two-dimensional donor,[16] actual for the 2D system, considered here. For both systems a monotonous increase of widths of levels at increasing electric-field strengths is characteristic for a domain of strong fields. The latter condition is satisfied for all the excited states in Coulomb potentials for both 2D and 3D cases for all the field strengths considered here and in Refs. 9 and 11–13.

More realistic explanation can be obtained by means of an analysis of the motion of the electron between the potential wells. It is easy to verify that for large R values the sequences of positions of maxima and minima in considered curves correspond to the asymptotic behavior of the Airy function, which is the solution of the Schrödinger equation for an electron in a uniform electric field. They look like[25,32]

$$\psi(z)=AM(\xi)e^{-i\Theta(\xi)},$$

$$\xi=\left(z+\frac{E}{F}\right)(2F)^{1/3}, \tag{7}$$

where $M(\xi)$ and $\Theta(\xi)$ are the modulus and phase of the Airy function, and A is a constant. The asymptotics of ψ for $z\to+\infty$ has the form

$$\psi(z)=\frac{A}{\sqrt{\pi}}\xi^{-1/4}\exp\left(-i\frac{\pi}{4}+i\frac{2}{3}\xi^{3/2}\right)+O(\xi^{-13/4}). \tag{8}$$

Except domains of small R values the oscillating curves in Figs. 1 and 3–12 look like the function (8) with $z=R$ and

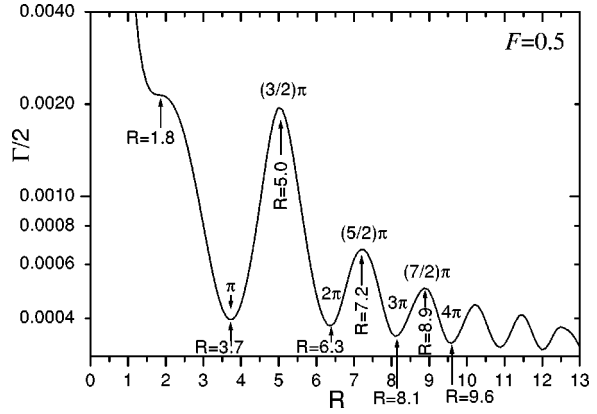

FIG. 12. Imaginary part of the energy of state $2p\sigma_u$ in a two-dimensional system of two Coulomb centers as functions of the distance R between the centers. $F=0.5$. The numbers over the maxima and minima give the phase shifts of corresponding wave functions (Fig. 13) between the two centers. Effective atomic units.

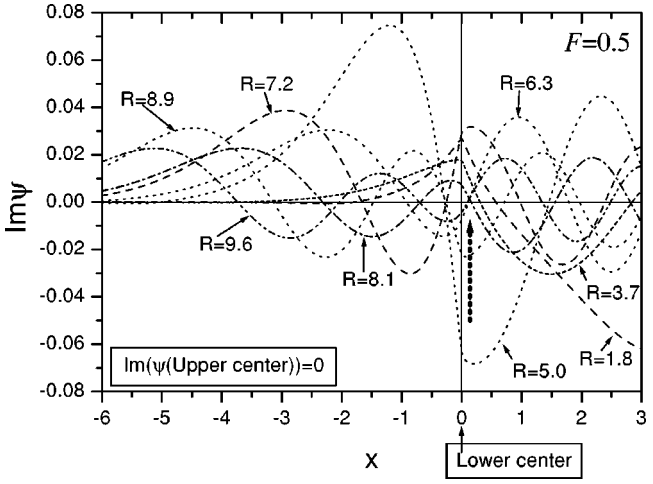

FIG. 13. Imaginary parts of the wave function of state $2p\sigma_u$ in a two-dimensional system of two Coulomb centers for several maxima and minima of the function $\Gamma/2(R)$ for $F=0.5$. $x=0$ is the position of the lower nucleus and $x=-R$ is the position of the upper nucleus. Effective atomic units.

with some additional amplitude multipliers and shifts. Equations (7) and (8) immediately provide the dependence of the width of maxima in these curves proportional to $\sqrt{F}$. An evident connection of the considered phenomenon with a phase shift of the wave function of an electron passing the segment between two potential wells leads to an explanation of this as an effect of an interference between an incident electronic wave dropping onto the lower Coulomb center and a reflected electronic wave. Dependent on the phase shift between the two centers an interaction of these waves leads either to an increase or to a decrease of the density of the electronic flux leaving the system. The latter is associated directly with the $\Gamma/2$ value.

To prove the above assumption we have carried out an investigation of a relation between the amplitude of $\Gamma(R)$ and the form of the numerical wave function for various R values. Results of this investigation are presented in Figs. 12 and 13. In Fig. 12 we present the function $\Gamma(R)$ for state $2p\sigma_u$ at $F=0.5$ and mark the R values corresponding to several first maxima and minima in this curve. For these points we depict in Fig. 13 the profiles of the imaginary parts of the corresponding wave functions parallel to the ''molecular'' axis and lying close to it. To make the comparison of wave functions obtained for different R more convenient they are shifted along the x axis so that the position of the lower center corresponds to $x=0$ for all the R values. After this shift the upper center lies at the point $(x=-R,y=0)$. The wave functions are normalized by the condition $\mathrm{Im}\,\psi(x=-R,y=0)=0$. This condition allows reducing the calculation of the phase shift with respect to the position of the upper center to a simple counting of zeros and extrema of $\mathrm{Im}\,\psi$.

The investigation of interference phenomena in this system is much more complicated than in textbook examples of, e.g., the optical interference between two boundaries of media with different refraction coefficients or the behavior of a quantum particle between two potential barriers. Our problem is two dimensional, the wavelength depends on the spatial coordinates, and, the most important, the fields of the Coulomb centers cannot be considered like pointlike objects. This means that when considering the wave functions in Fig. 13 we cannot say that we consider interference of electronic waves at points $(-R,0)$ and $(0,0)$. The origin for calculating phase shifts is fixed in Fig. 13 at the point $(-R,0)$. On the other hand, it is more reasonable to expect *a priori* that effective positions of the second center forming a picture of the interference have to depend on the energy of the incident electron and cover some area in the vicinity of the lower Coulomb center. Nevertheless, for all the points marked in Fig. 12, except $R=1.8$, it is possible to find a small area playing the role of an effective center of the reflection for a broad range of R values (and, thus, for a broad range of energies of incident electrons). The position of this area is marked in Fig. 13 by a bold point arrow. Phase shifts between this small area and the point $(-R,0)$ are given in Fig. 12 at the corresponding maxima and minima. One can see that integer numbers of π correspond to minimal rates of ionization for the state $2p\sigma_u$. Half-integer numbers of π provide the highest probabilities for leaving the system for an electron, initially located near the upper Coulomb center.

It is reasonable to give here an example of a similar interference phenomenon, well known for many years. This is an elastic scattering of a particle by two atoms.[30] The sizes of atoms are supposed negligibly small compared with the distance R between them. As an analog of our problem one can consider a linear configuration, when the wave vector of the incoming particle is parallel to the line, connecting atoms. It follows from the simplest consideration given in Ref. 30 that the cross section of backward scattering has minima, when the difference of phases of the initial wave between positions of the two atoms is

$$\Delta\phi=\frac{\pi}{2}+\pi n, \tag{9}$$

where n is an integer number. The maxima of the cross section correspond to phase shifts

$$\Delta\phi = \pi n \tag{10}$$

between two atoms. In our problem it is reasonable to suppose that a maximum of the cross section for backward scattering corresponds to a maximal lifetime of the electron inside the system. This situation must correspond to a minimum of $\Gamma/2$. Analogously, condition (9) has to correspond to maxima of $\Gamma/2$. We see that these qualitative considerations agree with the analysis of the phase shifts of the wave function presented above. Both the phenomenon in question and the latter example could be characterized briefly either as an interference of the electronic wave on two centers or as a resonance phenomena in the two-center system.

It should be noted that the discussion of the oscillating character of $\Gamma/2(R)$ for the state $2p\sigma_u$ is based on one-dimensional models and cannot reproduce many other features of the numerical results obtained in our calculations. Some of these features we will discuss in the final part of this section.

Opposite to the state $2p\sigma_u$, dependencies $\Gamma/2(R)$ for state $1s\sigma_g$ do not contain any oscillations. This difference is an evident result of the fact that for $F>0$ the wave function of state $1s\sigma_g$ is localized in a vicinity of the lower Coulomb center and due to a high potential barrier owing to the term $-Fz$ in the Hamiltonian (2) the density of this wave function at the upper nucleus is negligible small. A smooth increase of the function $\Gamma/2(R)$ for state $1s\sigma_g$ results from a decrease of the binding energy of this state due to decreasing influence of the field of the upper Coulomb center as $R\to\infty$. In this limit the value of $\Gamma/2$ corresponds to the ground state of an electron in an isolated 2D Coulomb center.[16] The oscillating dependencies for the state $2p\sigma_u$ have the same limit. Relative positions of the curves for states $1s\sigma_g$ and $2p\sigma_u$ are different for regimes of the tunneling ($F<1$) and the overbarrier ionization ($F>1$). For weak fields and arbitrary R values the rate of ionization for state $2p\sigma_u$ is higher than for state $1s\sigma_g$. For small R this is due an evident difference in bound energies between the ground and the excited states. For large R values the cause consists in the fact that due to a long-range character of the Coulomb potential the potential barrier for tunneling of the $2p\sigma_u$ electron is lower and narrower than for the $1s\sigma_g$ electron (see Fig. 2). On the other hand, for an overbarrier ionization in strong electric fields the difference in the heights of potential barriers does not play an important role, and when the field strength increases, the oscillating curve for state $2p\sigma_u$ tends to oscillate around the curve for state $1s\sigma_g$.

Oscillations of $\Gamma/2(R)$ for state $2p\sigma_u$ are characteristic for relatively large distances between the Coulomb centers. Another type of behavior, not associated with oscillations of the wave function between centers, is better visible for lower intensities. For small R values one can see a fast decrease of the $\Gamma/2$ associated with a drop of the energy of the excited state $2p\sigma_u$. The next section of this dependence, clearly visible for $F=0.2$ (Fig. 4), is associated with increase of the height of the potential barrier separating the domain of a finite classical motion of the electron in the vicinity of a center and the domain of its infinite motion. This behavior is similar to that of the $1s\sigma_g$ state and in this section ($1.9<R<6.15$ for $F=0.2$) the dependencies for states $1s\sigma_g$ and $2p\sigma_u$ are approximately parallel. Due to a smaller height and spatial extension of the potential barrier for the state $2p\sigma_u$ the curve $\Gamma/2(R)$ for this state lies higher than that for the state $1s\sigma_g$. The maximum of the curve for $F=0.2$ at the point $R=6.15$ can be associated with a phase shift between centers equal to $\pi/2$. After this point the behavior of the function $\Gamma/2(R)$ changes and the wave function for the minimum at $R=8.66$ clearly demonstrates the phase shift equal to π.

The last feature of the function $\Gamma/2(R)$, which we have to explain here, is a faster damping of oscillations in a 3D system compared with the 2D one. The explanation consists in the much better possibilities for a spatial dissipation of an outgoing electronic wave in a 3D space compared with the 2D case. In result in the two-dimensional system considered above the electronic wave dropping from the upper center has larger density at the lower center than this takes place in a 3D system. As a result, the interference phenomena are more intensive in a 2D system than in a 3D one. This reasoning allows us to come to the conclusion that these interference phenomena are to be even better pronounced in one-dimensional systems, e.g., in quantum wires.

IV. TWO QUANTUM DOTS

In this section we consider a system of two quantum dots with potentials

$$V(x,y) = -A\exp[-(r/r_0)^2], \quad r=\sqrt{x^2+y^2}. \tag{11}$$

This form of the potential is close to a real potential existing in double quantum dots in GaAs/AlGaAs structures.[33] In this paper we do not give detailed calculations for parameters A and r_0 corresponding to some specific experimental situations and restrict our consideration by a model example allowing us to compare the behavior of an electron in the systems of two Coulomb centers and two quantum dots. In a more theoretical and mathematical aspect this comparison provides a possibility to get an idea about effects of long- (Coulomb) and short-range, Eq. (11), potentials in two-center systems in external electric fields.

To this end we carried out calculations for $A=5$ and $r_0=0.85$. In the field-free scenario this set of parameters provides the energy of the ground-state level in a separate quantum dot at $E=-2.003\,762$ and the first (and only) excited level at $E=-0.038\,964$. Such kind of a spectrum and a general form of the potential illustrated by Fig. 2 allow a direct comparison with calculations of the preceding section without changing scales of the energy, electric-field strengths, and R. The results of our calculations for $F=0.5$ are presented in Fig. 14.

One can see several features which distinguish the system of two quantum dots from the system of two Coulomb centers. For $R>3$ the real parts of energies of states $1s\sigma_g$ and

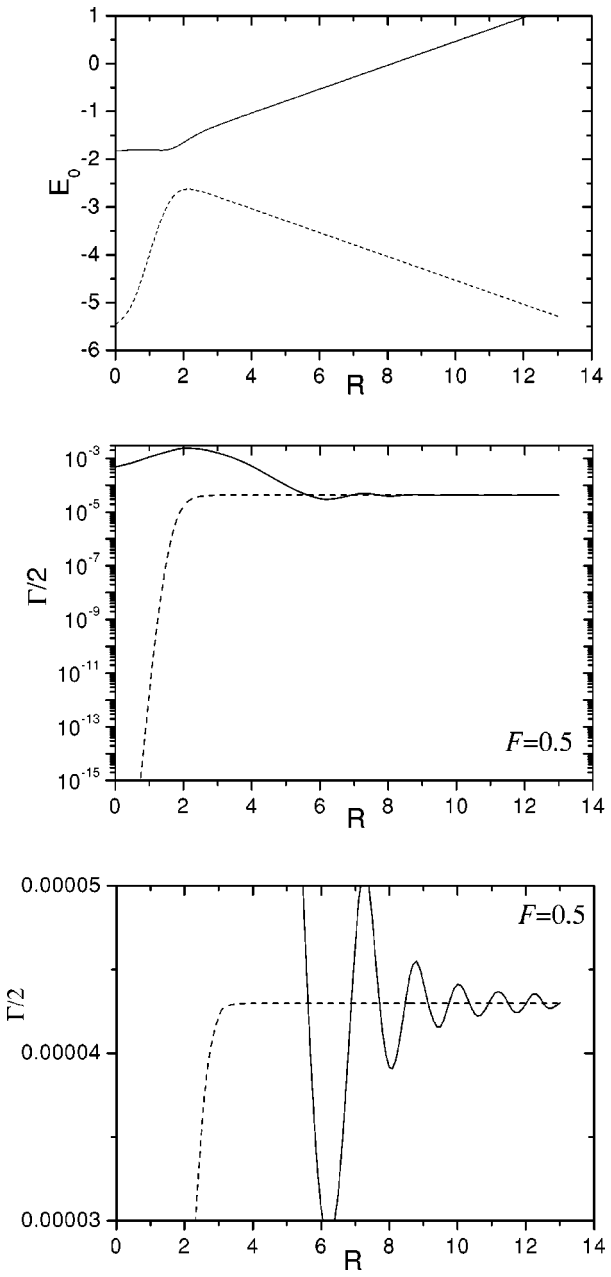

FIG. 14. Real and imaginary (two different scales) parts of the energy of an electron in a system of two quantum dots as functions of the distance R between them for $F=0.5$. States $1s\sigma_g$ and $2p\sigma_u$. Effective atomic units.

$2p\sigma_u$, presented in Fig. 14, have linear dependencies on R. This linearity is fulfilled with higher precision than in the case of two Coulomb centers (Fig. 2). On the other hand, the transformation of the behavior of $E_0(R)$ from the regime of separate potential wells to that of one united well $R<2$ happens also sharper than for two Coulomb centers. This feature is an evident result of the short-range character of potential (11), which is negligibly small for $R>3$. The sharp transition in the behavior of the imaginary part of state $1s\sigma_g$ from a fast increasing with growing R to a constant value independent of R taking place at $R\approx 3$ has the same origin. The function $\Gamma/2(R)$ for state $2p\sigma_u$, shown in Fig. 14 in two different scales, has similar character of oscillations with a periodicity very near to that for two Coulomb centers at the same F and R values. On the other hand, these oscillations decrease with increasing R faster than this happens for two Coulomb centers. The latter can be explained by a lower intensity of the $2p\sigma_u$ wave function at the lower nucleus for short-range potentials compared with a pair of Coulomb potentials. This is due to the fact that long-range Coulomb potentials form a kind of a channel preventing dissipation of the electronic density sidewards from the axis of the system. For small values of $|y|$ the potential in between the nuclei is clearly lower in the Coulomb system, as one can see in Fig. 2, whereas for large $|y|$ the difference between the Coulomb and the short-range potentials is much smaller.

V. CONCLUSIONS

We have calculated energies and lifetimes for two different two-dimensional analogs of the hydrogen molecular ion H_2^+ in external static electric fields directed along the axis of the system. Detailed calculations for a pair of Coulomb impurity centers in a narrow two-dimensional quantum well are carried out for a pair of states $1s\sigma_g$ and $2p\sigma_u$, which are the ground states of an electron for spatially separated Coulomb quantum wells. The calculations are performed for a broad range of electric-field strengths, including both the regime of the underbarrier tunneling of the electron and the overbarrier regime for the electron leaving the system. The dependencies $E_0(R)$ of the real parts of energies form at large R values an easily predictable fanlike picture. For strong electric fields these dependencies for the state $2p\sigma_u$ contain oscillations, corresponding to the much more visible oscillations of the imaginary part of the energy of this state. The latter are similar to oscillations obtained earlier for the state $2p\sigma_u$ of the hydrogen molecular ion.[9,11–13] The corresponding dependencies for the state $1s\sigma_g$ are simpler and do not exhibit any oscillations for $R\to\infty$. A specific feature of the two-dimensional system considered here consists in more pronounced and slower decreasing with R oscillations of dependencies for the $2p\sigma_u$ state as compared to the 3D case.

The phenomenon of nonmonotone dependencies for state $2p\sigma_u$ in the hydrogen molecular ion is usually referred to an interaction of a quasistationary state localized at one of the nuclei with broad resonance states at the second one. This argument does not explain the near to periodic character of the function $\Gamma(R)$ and decrease of its period with growing F values. We explain the oscillation picture by an interference of the electronic wave between two centers. This interpretation is confirmed by an analysis of phase shifts of the wave function between the positions of the centers. Thus, we can state that the phenomena considered above originate from a resonance behavior of the electronic waves in the molecularlike system as wholes and cannot be associated directly with properties of separate parts of the system. More pronounced oscillations are due to lesser spatial dissipation of the electronic wave in 2D systems compared to 3D ones.

The second system considered in this paper is a pair of

quantum dots with Gaussian attractive potentials. The behaviors of both real and imaginary parts of the energy for states $1s\sigma_g$ and $2p\sigma_u$ coincide with that for the case of Coulomb centers. Distinctions are due to the short-range character of the potential of quantum dots. The differences are a faster convergence of $\Gamma(R)$ to its limit as $R\to\infty$ for state $1s\sigma_g$ and faster decrease of oscillations of this dependence for state $2p\sigma_u$. The latter is due to the fact that long-range Coulomb potentials form a kind of a channel preventing dissipation of the electronic density sidewards from the axis of the system. Short-range Gaussian potentials do not form such a channel. In other words we can say that the resonances of the electronic wave between the two short-range potentials are less pronounced than between two Coulomb centers.

ACKNOWLEDGMENT

One of the authors (M.V.I.) gratefully acknowledges financial support by the Deutsche Forschungsgemeinschaft.

*Permanent address: Institute of Precambrian Geology and Geochronology, Russian Academy of Sciences, Nab. Makarova 2, St. Petersburg 199034, Russia. Electronic address: mivanov@mi1596.spb.edu

[1] G. Bastard, E.E. Mendez, L.L. Chang, and L. Esaki, Phys. Rev. B **28**, 3241 (1983).
[2] J.A. Brum, C. Priester, and G. Allan, Phys. Rev. B **32**, 2378 (1985).
[3] K. Tanaka, M. Kobashi, T. Shichiri, T. Yamabe, D.M. Silver, and H.J. Silverstone, Phys. Rev. B **35**, 2513 (1987).
[4] H. Chen, X. Li, and S. Zhou, Phys. Rev. B **44**, 6220 (1991).
[5] D.M. Larsen and S.Y. McCann, Phys. Rev. B **46**, 3966 (1992).
[6] M. Morifuji and C. Hamaguchi, Phys. Rev. B **58**, 12 842 (1998).
[7] G. Kioseoglou, H.D. Cheong, T. Yeo, H.A. Nickel, A. Petrou, B.D. McCombe, A.Yu. Sivachenko, A.B. Dzyubenko, and W. Schaff, Phys. Rev. B **61**, 5556 (2000).
[8] Z.X. Jiang, B.D. McCombe, and P. Hawrylak, Phys. Rev. Lett. **81**, 3499 (1998).
[9] Z. Mulyukov and R. Shakeshaft, Phys. Rev. A **63**, 053404 (2001).
[10] M.V. Ivanov, J. Phys. B **34**, 2447 (2001).
[11] T. Zuo and A.D. Bandrauk, Phys. Rev. A **52**, R2511 (1995).
[12] Z. Mulyukov, M. Pont, and R. Shakeshaft, Phys. Rev. A **54**, 4299 (1996).
[13] M. Plummer and J.F. McCann, J. Phys. B **29**, 4625 (1996); **30**, L401 (1997).
[14] R. Barnett and G.N. Gibson, Phys. Rev. A **59**, 4843 (1999).
[15] W. Kohn and J.M. Luttinger, Phys. Rev. **98**, 915 (1955).
[16] M.V. Ivanov and R. Schinke, J. Phys.: Condens. Matter **15**, 5909 (2003).
[17] M.V. Ivanov, Sov. Phys. Semicond. **19**, 1167 (1985); Zh. Vychisl. Mat. Mat. Fiz. **26**, 140 (1986); J. Phys. B **27**, 4513 (1994).
[18] M.V. Ivanov, J. Phys. B **21**, 447 (1988).
[19] M.V. Ivanov and P. Schmelcher, Adv. Quantum Chem. **40** (2), 361 (2001).
[20] M.V. Ivanov, Phys. Lett. A **239**, 72 (1998).
[21] M.V. Ivanov and P. Schmelcher, J. Phys. B **34**, 2031 (2001); Eur. Phys. J. D **14**, 279 (2001); Phys. Rev. A **61**, 022505 (2000); **60**, 3558 (1999); **57**, 3793 (1998).
[22] Opt. Spectrosc. **83**, 23 (1997).
[23] M.V. Ivanov and P. Schmelcher, Phys. Rev. B **65**, 205313 (2002).
[24] M.V. Ivanov, Opt. Spektrosk. **76**, 711 (1994) [Opt. Spectrosc. **76**, 631 (1994)].
[25] M.V. Ivanov, J. Phys. B **31**, 2833 (1998).
[26] M. V. Ivanov, in *Atoms, Molecules and Quantum Dots in Laser Fields: Fundamental Processes*, edited by N. Bloembergen, N. Rahman, and A. Rizzo [Editrice Compositori, Bologna, 2000 (Ital. Phys. Soc. Conf. Proc., **71**)], p. 301.
[27] V. Franceschini, V. Grecchi, and H.J. Silverstone, Phys. Rev. A **32**, 1338 (1985).
[28] L. Benassi and V. Grecchi, J. Phys. B **13**, 911 (1980).
[29] J.N. Silverman and C.A. Nicolaides, Chem. Phys. Lett. **153**, 61 (1988).
[30] A. Messiah, *Quantum Mechanics* (North-Holland, Amsterdam, 1969), p. 851.
[31] V.V. Kolosov, J. Phys. B **20**, 2359 (1987); **22**, 833 (1989).
[32] M. Abramowitz and I. A. Stegun, *Handbook of Mathematical Functions* (National Bureau of Standards, Washington, DC, 1964).
[33] N.A. Bruce and P.A. Maksym, Phys. Rev. B **61**, 4718 (2000); P.A. Maksym, H. Imamura, G.P. Mallon, and H. Aoki, J. Phys.: Condens. Matter **12**, R299 (2000).